

SOURCE LOCATION ESTIMATION USING PHASELESS MEASUREMENTS WITH THE MODULATED SCATTERING TECHNIQUE FOR INDOOR WIRELESS ENVIRONMENTS

J. H. Choi, B. Y. Park, and S. O. Park

Department of Information and Communications Engineering
Korea Advanced Institute of Science and Technology
103-6, Munji-Dong, Daejeon, 305-732, Republic of Korea

Abstract—This paper proposes the source location estimation technique with the modulated scattering technique (MST) for indoor wireless environments. The uniform circular scatterer array (UCSA) that consist of five optically modulated scatterers as array elements and a dipole antenna at the center of the UCSA is employed for estimating a source location from the impinging signal. In contrast with a conventional uniform circular array (UCA), the proposed method using the MST needs only one RF path. Also, the plane-wave assumption of the impinging signal is not necessary for an array signal processing because the proposed method is based on a phaseless measurement. Therefore, the proposed method can be applied in short-range LOS and NLOS environments that the plane-wave signal cannot be formed. A source location is estimated by using a simple estimation algorithm based on the power difference of the scattering signals modulated by two scatterers on the UCSA. The power difference is caused by different propagation loss between a source and each scatterer. The performance of the proposed method is demonstrated by measuring the angles of the incoming signals in the anechoic chamber and by comparing the estimated angles with the simulated results.

1. INTRODUCTION

For efficient utilization of spectral resources for various mobile services, smart antenna and adaptive array antenna technologies have been considered in smart base stations [1]. Also, they have been considered for WiMAX femto base stations and WiFi access points in indoor

Corresponding author: J. H. Choi (jhchoi05@kaist.ac.kr).

wireless environments [2, 3]. In many kinds of base stations, the direction-of-arrival (DOA) estimation and localization estimation techniques are very important issues for adopting a beam to a desired direction. The increase of spectral efficiency can be achieved by a beamforming technique without additional resources [4]. A source localization technique has the strong relation with the DOA estimation because the maximum intensity of the DOA spectrum can be thought as an incoming direction of the source.

Many kinds of estimation techniques have been investigated for a long time. Beamforming and Bartlett DOA estimation methods which are one of the earliest methods have been used due to its simplicity although resolution is limited by array's aperture size. Nowadays, the multi signal classification (MUSIC), estimation of signal parameters via rotational invariance technique (ESPRIT), and maximum likelihood (ML) have been used popularly in order to achieve high-resolution performance [5]. Based on angle-of-arrival (AOA), time-of-arrival (TOA), time-difference-of-arrival (TDOA), and received-signal-strength (RSS) techniques, a source localization technique have been investigated. Also, closed-form solutions based on a spherical intersection and a hyperbolic intersection have been used for a closed-form least squares source localization [6].

Recently, in contrast to a conventional array configuration, the DOA estimation method using electronically steerable parasitic array radiator (ESPAR) which has only one RF port has been investigated because of inexpensive hardware structures. Although the system using a ESPAR has many advantages, the lack of samples for constructing correlation matrices and phase calibration errors between the array elements degrade the estimation accuracy [7–12].

To mitigate a few disadvantages of the previous works and inherit their superiorities, the MST have been considered in this paper. The MST has been popularly used for rapid near-field measurement without scarifying the acceptable level of accuracy [13]. In order to characterize microwave fields at a probe's location with the amplitude and phase, the MST uses non-linear devices loaded on a short dipole scatterer with modulating at a low frequency [14, 15]. The MST have used several modulated scatterers placed at the pre-defined positions to increase the measurement speed and provide economical solution using a low frequency switch instead of an expensive RF switch [16, 17]. Incorporating the advantages of the MST, a source location estimation can be done effectively. Also, a source location estimation for indoor wireless environments like short-range LOS and NLOS environments can be possible because a plane-wave assumption is not necessary. A simple estimation algorithm for the proposed method utilizes only the

amplitude of the modulated scattering signals. The spherical-wave model has been studied for the accurate channel modeling without plane-wave assumption [18, 19].

This paper proposes the source location estimation method using the UCSA and the MST for indoor wireless environments, and shows the simple estimation algorithm for a single source using a phaseless measurement in an anechoic chamber with no plane-wave assumption. The measured incoming angles of the sources using the proposed method are compared with the simulated incoming angles for validation.

2. UNIFORM CIRCULAR SCATTERER ARRAY

The UCSA used in the proposed method is described in Fig. 1. The configuration of the UCSA is similar with those of the conventional UCA that has monopole or dipole antennas as array elements [20–22]. The UCSA consists of equally spaced optically modulated scatterers in a circular rim and one dipole antenna which has omnidirectional radiation pattern in the azimuth plane. An optically modulated scatterer is a short dipole antenna that has a photodiode which is loaded at the center of the short dipole antenna and optically switched by a laser source. A dipole antenna for receiving modulated scattering signals by scatterers on the UCSA is located at the center of the UCSA and connected to a single RF port. A low frequency square pulse through an optical fiber feeds a photodiode for switching operation. This operation modulates scattering signals.

The key idea of the UCSA is the use of the MST and a phaseless measurement. Though the conventional UCA should have same number of RF paths with array elements and an RF switch for one receiver, the proposed architecture need only one RF path with an inexpensive low frequency switch for driving a low frequency square pulse to each laser source sequentially. When a square pulse feeds one laser diode, a modulated scattering signal by one scatterer can be received at the receiver. Consequently, the modulated scattering signals by scatterers at the specific position on the UCSA can be received by feeding a square pulse to a laser diode that is connected to the photodiode of the scatterer. It seems that RF paths are being switched virtually by switching a low frequency square pulse. The range of the angle of the incoming signal can be refined by investigating an angular position of the scatterer that yield the strongest scattered field because the received power level depends on the distance between a source and a scatterer. Through these mechanism, a simple manipulation for estimation a source location

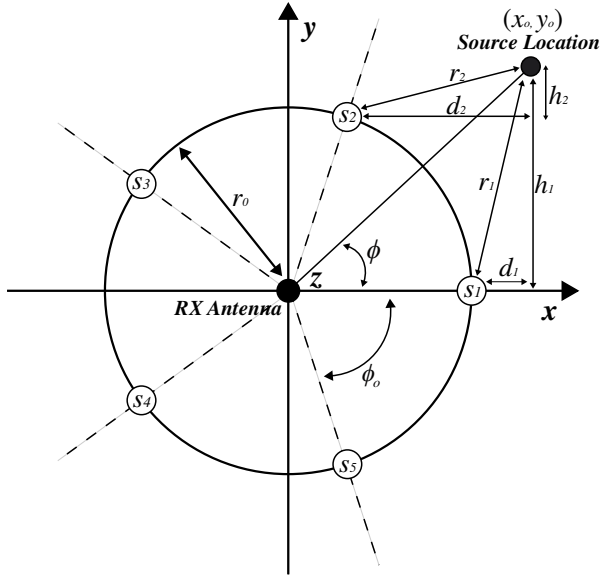


Figure 1. The geometry of an 5-element UCSA, scatterers are equally spaced on the x - y plane along the rim of a circle with radius r_o and one dipole antenna is at the center of the UCSA.

with phaseless modulated scattering signals can be possible. The estimation method will be discussed in the next section in detail.

3. PROPAGATION LOSS MODEL

For an M -element UCSA shown in Fig. 1, we assume that the origin is the coordinates of the UCSA's center, (x_o, y_o) represent the coordinate of the ideal point source for the propagation loss modeling and ϕ is the azimuthal angle of a source. The relative spacing angle between adjacent elements is given by

$$\phi_o = \frac{2\pi}{M} \quad (1)$$

where M is the number of array elements.

The distance r_n from a source and each scatterer can be written as

$$\left. \begin{aligned} r_n &= \sqrt{d_n^2 + h_n^2} \\ d_n &= x_o - r_o \cos \{(n-1) \cdot \phi_o\} \\ h_n &= y_o - r_o \sin \{(n-1) \cdot \phi_o\} \end{aligned} \right\}, \quad n = 1, 2, \dots, M \quad (2)$$

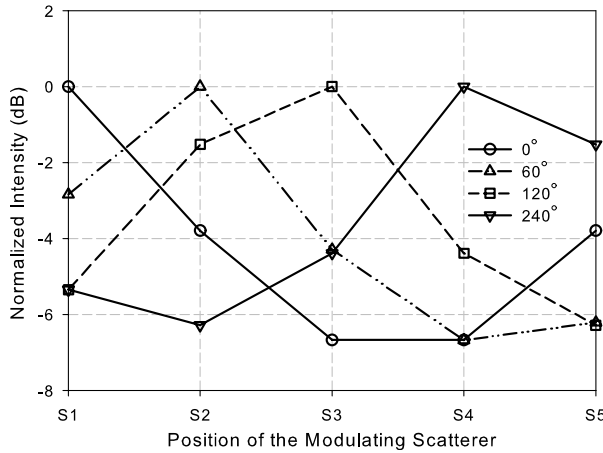


Figure 2. The simulated intensities of the received signals via each scatterer when a source impinges the UCSA from specific angles.

where n is the index of a scatterer, d_n is the distance between a source and the n -th scatterer along the x -axis, and h_n is the distance along the y -axis.

The received power P_r of the scattering signal modulated by the n -th scatterer can be simply modeled by Friis transmission equation as [23]

$$P_r(\text{dBm}) = P_t(\text{dBm}) + G_t(\text{dB}) + G_r(\text{dB}) - L_p(\text{dB}) + \alpha(\text{dB}) \quad (3)$$

where P_t is the transmitter power, G_t and G_r are the transmit and receive antenna gains, L_p is the propagation loss, and α is the ratio between the received signal by a scatterer as a short dipole and the scattering signal modulated by a scatterer in the bistatic setup [24].

The propagation loss in (3) can be modeled as

$$L_p(\text{dB}) = 10 \log \left(\frac{4\pi}{\lambda} \right)^2 + 10 \log (r^2) \quad (4)$$

where r is the distance between a source and each scatterer and λ is the wavelength because the received power in the radiating near-field and far-field regions strongly depends on the square of the separation distance.

Figure 2 shows the simulated intensities of the received signals traveling from a source to a receiving antenna via each scatterer using (2) and (3) when the wavelength of the source is about 11.5 cm at 2.6 GHz, M is 5, P_t is 15 dBm, and the incoming angle of the source is 0° , 60° , 120° , and 240° , respectively. In this paper, the exact values

of α , G_t , and G_r are not considered because the values are eliminated in a source location estimation procedure.

For example, in case of 60° shown in Fig. 2, the receiving signal via the scatterer placed at position S_2 has the highest intensity because it is inversely proportional to r^2 . That is, the angular position of the scatterer may close to that of the impinging signal because intensity should become higher as the propagation distance become shorter. It is the same situation that a square pulse feeds the laser diode that is connected to the photodiode on the scatterer at position S_2 . The power differences of the modulated scattering signals is the primary factor for a source location estimation algorithm.

4. SOURCE LOCATION ESTIMATION ALGORITHM

The mobile location in a real propagation environment can be estimated by using the difference of signal attenuations along two paths [25–27]. In same manner, a source location can be estimated by the power difference of the scattering signals modulated by two scatterers.

By propagation loss model in (3), the power difference of the scattering signals modulated by the i -th and j -th scatterers is given by [23]

$$P_i(\text{dBm}) - P_j(\text{dBm}) = 10 \log \left(\frac{r_j}{r_i} \right)^2, \quad i \neq j \quad (5)$$

where P_i and P_j are the received signals when a square pulse feeds the laser diode that is connected to the i -th and j -th scatterers sequentially, r_i and r_j are the distances between a source and the i -th and j -th scatterers. The ratio of the distances of propagation paths k_{ij} can be obtained by the power difference of the received scattering signals modulated by the i -th and j -th scatterers.

$$k_{ij} = \frac{r_j}{r_i} = 10^{\frac{P_i - P_j}{20}} \quad (6)$$

From (6), a possible source location can be expressed as

$$(x - x_j)^2 + (y - y_j)^2 = k_{ij}^2 \left\{ (x - x_i)^2 + (y - y_i)^2 \right\} \quad (7)$$

where (x, y) is the coordinates of the possible source location, (x_i, y_i) is the coordinates of the i -th scatterer, and (x_j, y_j) is the coordinates of the j -th scatterer. Finally, a circle equation that indicates a possible location of a source can be obtained from (7)

$$(x - x_{ij})^2 + (y - y_{ij})^2 = r_{ij}^2 \quad (8)$$

where (x_{ij}, y_{ij}) are the center coordinate of a circle and r_{ij} is the radius of this circle. The circle with central in (x_{ij}, y_{ij}) and radius r_{ij} can be represented by k_{ij} and the coordinates of the i -th and j -th scatterers through (9)–(11).

$$x_{ij} = \frac{k_{ij}^2 x_i - x_j}{k_{ij}^2 - 1}, \tag{9}$$

$$y_{ij} = \frac{k_{ij}^2 y_i - y_j}{k_{ij}^2 - 1}, \tag{10}$$

$$r_{ij} = \frac{k_{ij}}{(k_{ij}^2 - 1)} \sqrt{(x_i - x_j)^2 + (y_i - y_j)^2}. \tag{11}$$

A possible location for the source is the intersection of two circles that are drawn by three combinations of the received signals. Fig. 3 shows three circles and intersections with combination of power differences between the scattering signals by three scatterers at positions $S_1, S_2,$ and S_3 . A intersection inside the UCSA is a trivial point.

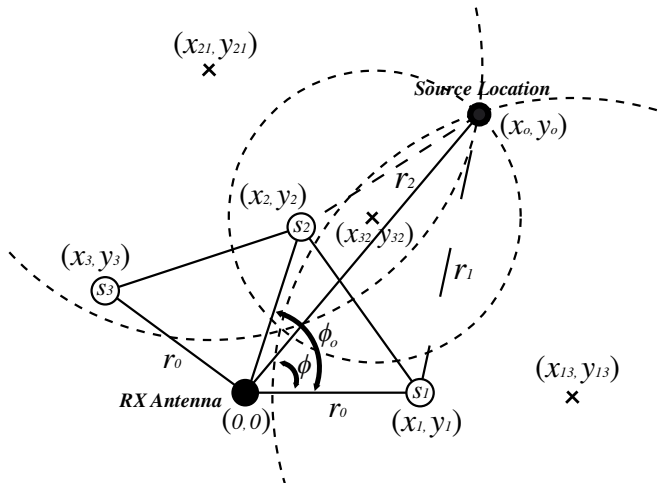


Figure 3. Illustration of positions of each scatterer, center of each circle and intersections of three circles pictured by power difference of scattered waves from the scatterers located at positions $S_1, S_2,$ and S_3 .

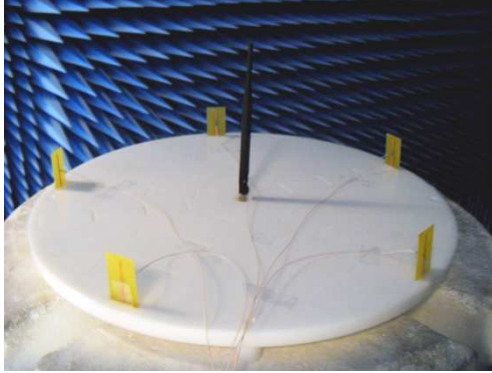


Figure 4. The fabricated UCSA with five optically modulated scatterers and a dipole antenna at the center.

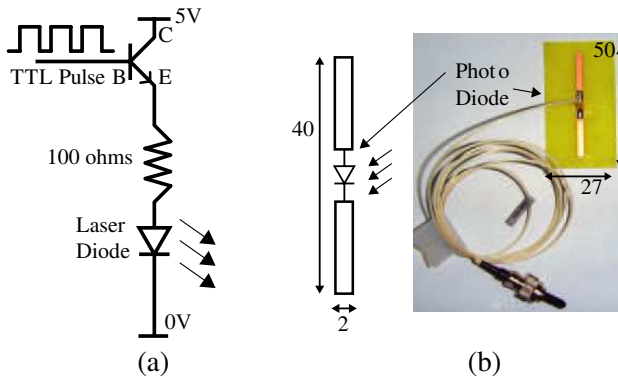


Figure 5. The configuration of (a) a driving circuit for a laser diode, (b) a modulated scatterer.

5. MEASUREMENT SETUP

The fabricated UCSA is depicted in Fig. 4. The UCSA has five optically modulated scatterers on a circle of radius 2λ at 2.6 GHz. A optically modulated scatterer shown in Fig. 5(b) is a strip dipole loaded by InGaAs photodiode (FD50S7). It was mounted on a FR4 substrate with relative permittivity of 4.6, thickness of 1 mm, width of 27 mm, and length of 50 mm. The width and height of a strip dipole are 2 mm and 40 mm which height is corresponding to a half wavelength at 2.6 GHz. A 7 kHz modulated laser optical signal generated by a driving circuit shown in Fig. 5(a) fed a photodiode to modulate a scattering

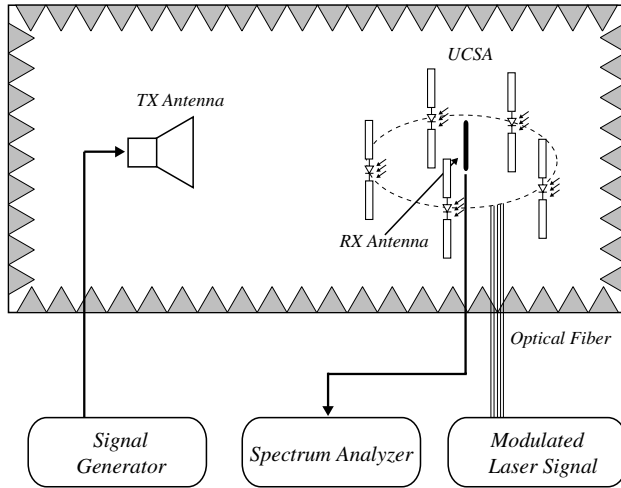


Figure 6. The configuration of the measurement system, and the locations of TX antenna and the UCSA in the anechoic chamber.

signal. A square pulse which has a TTL signal level was driven to five laserdiode driving circuits sequentially.

The configuration of the measurement system is shown in Fig. 6. A double-ridged horn antenna ($0.8 \sim 11$ GHz) was used as the TX antenna. A signal from the TX antenna is a single frequency of 2.6 GHz with the power of 10 dBm (Agilent E8358A). The UCSA is placed at the RX part as the RX antenna. A dipole antenna at the center of the UCSA was connected to the spectrum analyzer (Agilent E4403B) to receive a modulated scattering signal. The distance between the TX and RX antennas is 0.6 m. At this distance, the RX antenna is in the radiating near-field region where the wavefront is not planar. The 2-dimensional antenna measurement facility in the anechoic chamber was used in order to change a source direction. Instead of rotating the TX antenna, the rotational positioner in the RX part adjusted a receiving angle of the UCSA. It can be considered that the source direction is changed. The amplitude of the scattered signals which were sequentially modulated by all scatterers were measured by varying an angle of the incoming signal from positions S_1 to S_2 with angular resolution steps of 6° . Each measurement was accomplished by averaging 10 scattering samples modulated by the same scatterer.

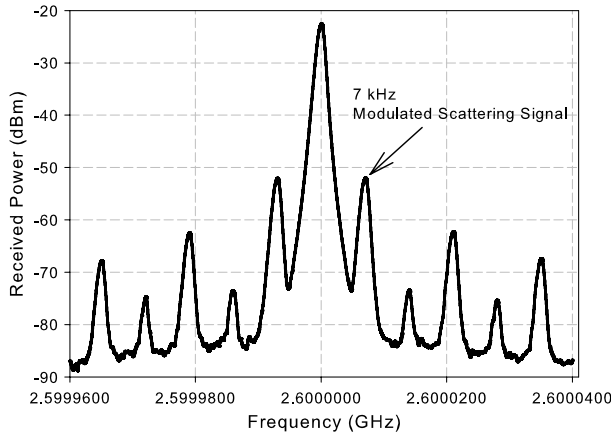


Figure 7. The measured spectrum of a modulated scattering signal when the direction of the source signal is 0 degree and a scattering signal is modulated by the scatter at position S_1 .

6. RESULTS AND DISCUSSION

For validation of the propagation loss model and the source location estimation method, simulations and measurements of the receiving signals scattered by each scatterer located at positions from S_1 to S_5 are presented. Also, the estimated incoming angles of the sources from simulations and measurements are presented.

The measured spectrum of a modulated scattering signal when the direction of the source signal is 0 degree and a scattering signal is modulated by the scatter at position S_1 is shown in Fig. 7. In the measurement, SNR between the modulated scattering signal and the noise floor is about 35.3 dB. However, actual SNR is 21.1 dB because the modulated signal is partially overlapped with the carrier signal of 2.6 GHz. A modulated component of $2.6 \text{ GHz} \pm 7 \text{ kHz}$ can be easily extracted from a single carrier frequency.

The simulated and measured signals scattered by the UCSA with respect to various angles of the incoming signals are shown in Fig. 8 and Fig. 9. The simulated results were normalized to the maximum received power for comparisons. Because the envelope of the received signal at the specific angle is very similar with the envelope at the slightly different angle, it is hard to discriminate two envelopes shown in the same graph. For clear comparisons, various angles between positions S_1 and S_2 are categorized into four groups, $(0^\circ, 24^\circ, 48^\circ)$, $(6^\circ, 30^\circ, 54^\circ)$, $(12^\circ, 36^\circ, 60^\circ)$, $(18^\circ, 42^\circ, 66^\circ)$.

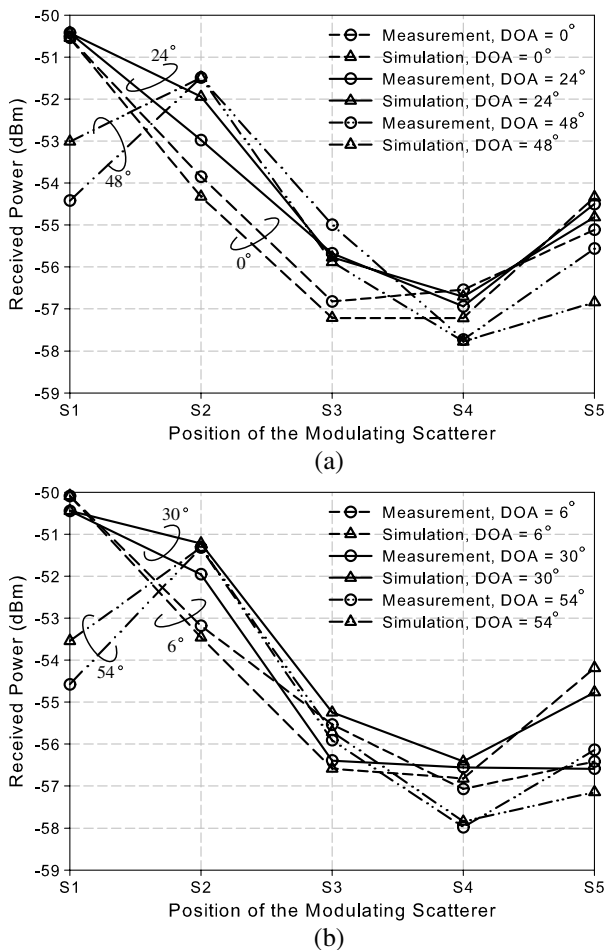


Figure 8. Comparison of simulated and measured received power of the scattered signals modulated by sequential feeding the modulated laser signals to each scatterer when the incoming angle of the source is (a) 0°, 24°, 48°, (b) 6°, 30°, 54°.

The simulated results have good agreements with the measured results. There are slight discrepancies between them because of non-ideal omnidirectional radiation pattern of an optically modulated scatterer, the presence of the central receiving antenna as an obstacle, and non-symmetric radiation pattern of the TX antenna. These factors are not considered in the propagation loss model. In case of 48°, shown in Fig. 8(a), the highest power is observed when a square pulse feeds

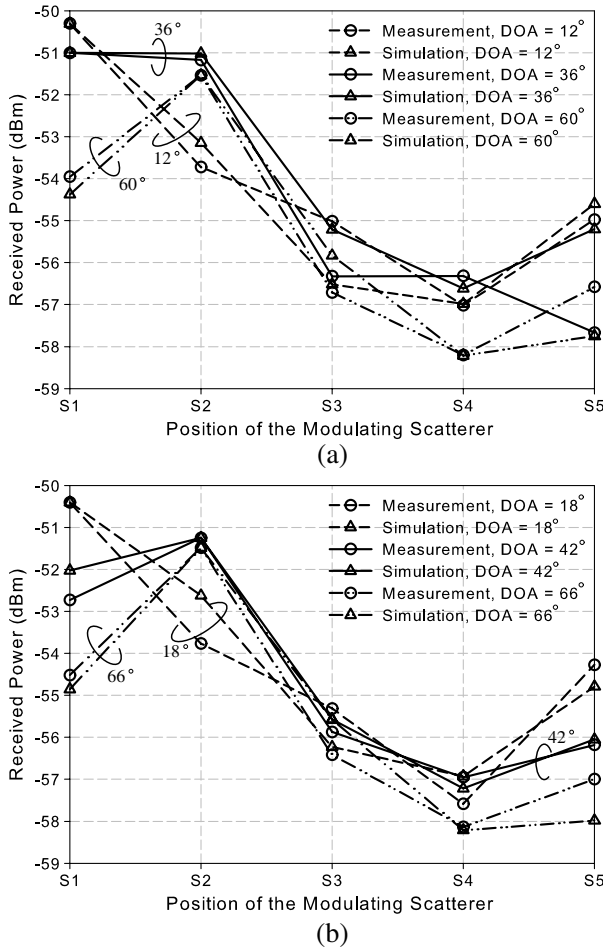


Figure 9. Comparison of simulated and measured received power of the scattered signals modulated by sequential feeding the modulated laser signals to each scatterer when the incoming angle of the source is (a) 12° , 36° , 60° , (b) 18° , 42° , 66° .

the laser diode that is connected to the photodiode on the scatterer at position S_2 . As mentioned in the previous section, possibility to find the exact angle of the source near the angular position of S_2 becomes very high. This principle gives us the proper range of the incoming angles of the source.

The estimated angles with the simulated and measured results are shown in Table 1. In case of simulations, the estimated results are

Table 1. The estimated incoming angles of the source with simulations and measurements.

Arrival Angle	Simulations		Measurements		
	DOA	Error	Range	DOA	Error
0	0.117	0.117	$0 - \frac{\phi_o}{2} \leq \phi \leq 0 + \frac{\phi_o}{2}$	2.453	2.453
6	5.954	0.046	$0 - \frac{\phi_o}{2} \leq \phi \leq 0 + \frac{\phi_o}{2}$	9.079	3.079
12	12.023	0.023	$0 - \frac{\phi_o}{2} \leq \phi \leq 0 + \frac{\phi_o}{2}$	12.254	0.254
18	17.936	0.064	$0 - \frac{\phi_o}{2} \leq \phi \leq 0 + \frac{\phi_o}{2}$	1.074	16.926
24	24.032	0.032	$0 - \frac{\phi_o}{2} \leq \phi \leq 0 + \frac{\phi_o}{2}$	16.505	7.495
30	29.987	0.013	$0 - \frac{\phi_o}{2} \leq \phi \leq 0 + \frac{\phi_o}{2}$	20.936	9.064
36	35.856	0.144	$0 - \frac{\phi_o}{2} \leq \phi \leq 0 + \frac{\phi_o}{2}$	35.025	0.975
42	41.984	0.016	$72 - \frac{\phi_o}{2} \leq \phi \leq 72 + \frac{\phi_o}{2}$	45.575	3.575
48	48.006	0.006	$72 - \frac{\phi_o}{2} \leq \phi \leq 72 + \frac{\phi_o}{2}$	58.290	10.29
54	54.045	0.045	$72 - \frac{\phi_o}{2} \leq \phi \leq 72 + \frac{\phi_o}{2}$	55.775	1.775
60	60.401	0.401	$72 - \frac{\phi_o}{2} \leq \phi \leq 72 + \frac{\phi_o}{2}$	44.166	15.834
66	65.996	0.004	$72 - \frac{\phi_o}{2} \leq \phi \leq 72 + \frac{\phi_o}{2}$	50.228	15.772
72	71.903	0.097	$72 - \frac{\phi_o}{2} \leq \phi \leq 72 + \frac{\phi_o}{2}$	77.304	5.304

* all units are degree.

perfectly close to the actual angles because power differences can be extracted exactly from the propagation loss model. The mean of the estimated error is 0.075° , the maximum is 0.401° , and the standard deviation is 0.1067° .

In case of measurements, power differences include the measurement errors due to unexpected factors in a real environment. By those reason, the obtained intersections indicate a wrong position and a few of combinations of circles may not have intersections. We can overcome measurement errors and increase estimation accuracy by defining the range of incoming angles and by averaging the estimated angles within this range. The possible range of incoming angles is determined by the angular position of the scatterer that yield the highest scattering signal. When the highest scattering signal is generated by the scatterer located at position S_1 , the possible range of incoming angles is from -36° to 36° . When the highest scattered signal is generated by the scatterer located at position S_2 , the possible range is from 36° to 108° . The mean of estimated error is 7.138° , the maximum is 16.926° , and the standard deviation is 5.974° .

7. CONCLUSION

In this paper, we examined the proposed source location estimation method based on the MST with a UCSA for indoor wireless environments. In the measurement system, the UCSA was used to modulate and re-radiate the received signals from a single source and one dipole antenna at the center of the UCSA was used for reception of sequentially modulated scattering signals by the UCSA. The incoming angle of the source can be estimated by power differences of the received scattering signals modulated by two scatterers of the UCSA. Consequently, it need only one RF path instead of using expensive RF switches and lots of receivers. Also, the proposed method employed a simple and low computational complexity algorithm with phaseless measurements because a plane-wave assumption is not necessary. As a result, the proposed system can be applied for a source location estimation for indoor wireless environments like short-range LOS and NLOS environments that the plan-wave cannot be formed. We have achieved good agreements between the actual incoming angles and the estimated angels by the proposed method.

ACKNOWLEDGMENT

This work was supported by the Korea Science and Engineering Foundation (KOSEF) through the Acceleration Research Program funded by the Ministry of Education, Science and Technology (MEST), Korea under contract No. 20090063501.

REFERENCES

1. Bellofiore, S., J. Foutz, C. A. Balanis, and A. S. Spanias, "Smart-antenna system for mobile communication networks, part 2, beamforming and network throughput," *IEEE Antennas and Propagation Magazine*, Vol. 44, No. 4, 106–114, Aug. 2002.
2. Kim, R. Y., J. S. Kwak, and K. Etemad, "WiMAX femtocell: requirements, challenges, and solutions," *IEEE Communications Magazine*, Vol. 47, No. 9, 84–91, Sep. 2009.
3. Chandrasekhar, V., J. Andrews, and A. Gatherer, "Femtocell networks: A survey," *IEEE Communications Magazine*, Vol. 46, No. 9, 59–67, Sep. 2008.
4. Godara, L., "Apprication of antenna arras to mobile communications, part II: Beam-forming and direction-of-arrival considerations," *Proceedings of the IEEE*, Vol. 85, No. 8, 1195–1245, 1997.

5. Krim, H. and M. Viberg, "Two decades of array signal processing research," *IEEE Signal Processing Magazine*, Vol. 13, No. 4, 67–94, Jul. 1996.
6. Chen, J. C., Y. Kung, and R. E. Hudson, "Source localization and beamforming," *IEEE Signal Processing Magazine*, Vol. 19, No. 2, 30–39, Mar. 2002.
7. Taillefer, E., A. Hirata, and T. Ohira, "Direction-of-arrival estimation using radiation power pattern with an ESPAR antenna," *IEEE Trans. Antennas and Propagation*, Vol. 53, No. 2, 678–684, 2005.
8. Plapous, C., J. Cheng, E. Taillefer, A. Hirata, and T. Ohira, "Reactance domain MUSIC algorithm for electronically steerable parasitic array radiator," *IEEE Trans. Antennas and Propagation*, Vol. 52, No. 12, 3257–3264, 2004.
9. Hwang, S., S. Burintramart, T. K. Sarkar, and S. R. Best, "Direction of arrival (DOA) estimation using electrically small tuned dipole antennas," *IEEE Trans. Antennas and Propagation*, Vol. 54, No. 11, 3292–3301, 2006.
10. Sun, C. and N. C. Karmakar, "Direction of arrival estimation with a novel single-port smart antenna," *EURASIP Journal on Applied Signal Processing*, Vol. 2004, No. 9, 1364–1375, 2004.
11. Taillefer, E., W. Nomura, and M. Taromaru, "New direction-of-arrival estimation method based on the reactance-domain ESPRIT algorithm with improved subarray-configuration selection," *The 9th European Conference of Wireless Technology*, 55–58, 2006.
12. Wu, Y. and H. C. So, "Simple and accurate two-dimensional angle estimation for a single source with uniform circular array," *IEEE Antenna Wireless Propagat. Lett.*, Vol. 7, 78–80, 2008.
13. Hygate, G. and J. F. Nye, "Measuring fields directly with an optically modulated scatterer," *Measure. Sci. Technol.*, Vol. 1, 703–709, 1990.
14. Choi, J. H., J. I. Moon, and S. O. Park, "Measurement of the modulated scattering microwave fields using dual-phase lock-in amplifier," *IEEE Antenna Wireless Propagat. Lett.*, Vol. 3, 340–343, 2004.
15. Bolomey, J. C. and F. E. Gardiol, *Engineering Applications of the Modulated Scatterer Technique*, Artech House, Norwood, MA, 2001.
16. Bolomey, J. C., B. J. Cown, G. Fine, L. Jofre, M. Mostafavi, D. Picard, J. P. Estrada, P. G. Friederich, and F. L. Cain, "Rapid near-field antenna testing via arrays of modulated scattering

- probes,” *IEEE Trans. Antennas and Propagation*, Vol. 36, No. 6, 804–814, Jun. 1988.
17. Qiang, C., K. Sawaya, T. Habu, and R. Hasumi, “Simultaneous electromagnetic measurement using a parallel modulated probe array,” *IEEE Trans. Electromagn. Compat.*, Vol. 49, 263–269, 2007.
 18. Jiang, J. S. and M. A. Ingram, “Spherical-wave model for short-range MIMO,” *IEEE Trans. Commun.*, Vol. 53, No. 9, 1534–1541, 2005.
 19. Bohagen, F., P. Orten, and G. E. Oien, “On spherical vs. plane wave modeling of line-of-sight MIMO channels,” *IEEE Trans. Commun.*, Vol. 57, No. 3, 841–849, 2009.
 20. Balanis, C. A., *Antenna Theory, Analysis, and Design*, 2nd edition, Wiley, New York, 1997.
 21. Mathews, C. P. and M. D. Zoltowski, “Eigenstructure techniques for 2-D angle estimation with uniform circular arrays,” *IEEE Trans. Signal Process.*, Vol. 42, No. 9, 2395–2407, Sep. 1994.
 22. Du, K. L., “Pattern analysis of uniform circular array,” *IEEE Trans. Antennas and Propagation*, Vol. 52, No. 4, 1125–1129, 2004.
 23. Lazaro, A., D. Girbau, and D. Salinas, “Radio link budgets for UHF RFID on multipath environments,” *IEEE Trans. Antennas and Propagation*, Vol. 57, No. 4, 1241–1251, 2009.
 24. Azaro, R., S. Caorsi, and M. Pastorino, “On the relationship for the bistatic modulated scattering technique in scattering applications using scattering properties of antennas,” *IEEE Trans. Antennas and Propagation*, Vol. 46, 1399–1400, Sep. 1998.
 25. Lin, D. and R. Juang, “Mobile location estimation based on differences of signal attenuations for GSM systems,” *IEEE Trans. Vehicular Tech.*, Vol. 54, No. 4, 1447–1454, 2005.
 26. Lin, H., S. Chen, D. Lin, and H. Lin, “Multidimensional scaling algorithm for mobile location based on hybrid SADOA/TOA measurement,” *IEEE Wireless Communications and Networking Conference*, 3015–3020, 2008.
 27. Caffery, J. J., “A new approach to the geometry of TOA location,” *Proc. IEEE Vehicular Tech. Conference*, Vol. 4, 1943–1949, 2000.